Analytica Chimica Acta 1174 (2021) 338747

Contents lists available at ScienceDirect

Analytica Chimica Acta

journal homepage: www.elsevier.com/locate/aca

Hydrazone ligation assisted DNAzyme walking nanomachine coupled with CRISPR-Cas12a for lipopolysaccharide analysis

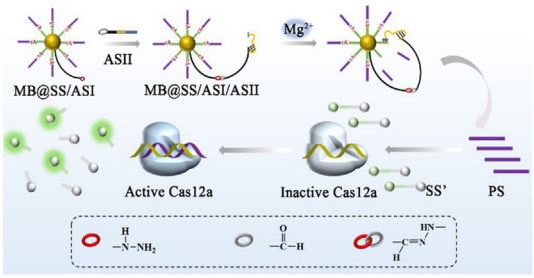
Pei Wang [a], Yamei Liu [a], Ying Yu [b], Yuan Zhang [a], Jinhui Peng [c], Lili Niu [a, **], Juan Zhang [a, *]

[a] School of Life Sciences, Shanghai University, Shanghai, 200444, PR China
[b] Department of Food Science and Engineering, School of Agriculture and Biology, Shanghai Jiao Tong University, Shanghai, 200240, China
[c] Department of Joint Surgery and Orthopedic Medicine, Shanghai Changzheng Hospital, Second Military Medical University, Shanghai, 200003, PR China

HIGHLIGHTS

- Hydrazone ligation assisted DNAzyme walking nanomachine has been coupled with CRISPR-Cas12a system.
- Hydrazone ligation with high efficiency can improve the performance of DNAzyme walking nanomachine.
- Cascade signal amplification can be realized to significantly improve the detection sensitivity.
- Cascade signal amplification has been further developed as a biosensor to analyze lipopolysaccharides.
- This work provides a new perspective for cascade signal amplification based on CRISPR-Cas system.

GRAPHICAL ABSTRACT



ARTICLE INFO

Article history:
Received 7 April 2021
Received in revised form
24 May 2021
Accepted 6 June 2021
Available online 8 June 2021

Keywords:
Cascade signal amplification
CRISPR-Cas12a
DNAzyme walker
Hydrazone ligation
Lipopolysaccharide

ABSTRACT

In this work, hydrazone ligation assisted DNAzyme walking nanomachine is explored to couple with CRISPR-Cas12a *trans*-cleavage. Hydrazone ligation with high efficiency can mediate signal input which can be induced by target binding, thereby regulating the performance of DNAzyme walking nanomachine. The product strand from DNAzyme walking nanomachine can further activate the *trans*-cleavage of Cas12a. So, cascade signal amplification can be achieved to enhance the sensitivity for target detection. Subsequently, hydrazone ligation assisted DNAzyme walking nanomachine coupled with CRISPR-Cas12a has been further developed as a biosensor to analyze lipopolysaccharides. The developed biosensor exhibits a linear range from 0.05 ng/mL to 10^6 ng/mL and a lowest limit of detection of 7.31 fg/mL. This research provides a new mode for the signal output of DNAzyme walking nanomachine, so as to sensitively analyze different biomolecules.

© 2021 Elsevier B.V. All rights reserved.

1. Introduction

As one kind of dynamic DNA nanomachine, DNA walking nanomachine has attracted widespread attention owning to its predictable molecular behavior and the characteristics of progressivity and movability [1]. The three-dimensional DNA walking nanomachine owns admirable signal amplification capability resulting from the high surface-to-volume ratio of nanoparticle

* Corresponding author.
** Corresponding author.
E-mail address: juanzhang@shu.edu.cn (J. Zhang).

https://doi.org/10.1016/j.aca.2021.338747
0003-2670/© 2021 Elsevier B.V. All rights reserved.

[2,3]. In general, the driving force of DNA walking nanomachine mainly depends on DNA strand, enzyme and even pH value [2,4,5]. Among them, metal ion-depended DNAzyme exhibits great potential as a driving force. In addition, chemoselective reaction such as hydrazone chemistry has been explored as the driving force to mediate the operation of DNA walking nanomachine by our group [6]. Herein, a novel hydrazone ligation assisted DNAzyme walking nanomachine has been developed with its multi-functionality [7]. Currently, the signal output mode of DNAzyme walking nanomachine is mainly direct output of fluorescence or electrochemical signal resulting from far away of short signal probe strand from gold nanoparticle or electrode interface [8–11]. In this work, an indirect signal output mode can be developed with the assistance of CRISPR-Cas12a system.

Clustered regulatory interspaced short palindromic repeats (CRISPR)-Cas is an adaptive immune mechanism formed in the long-term evolution of bacteria. When the activated Cas nucleases cuts the target strand, it will also cut the nearby non target strand indiscriminately at the same time [12–15]. Thereby, the system plays a key role in both gene editing and analytical detection [16–20]. Among them, CRISPR-Cas12a (Cpf1) activated by CRISPR RNA (CrRNA), can cleave the target DNA and any nontarget single strand DNA (ssDNA) [15,21]. The dual-labeled nontarget ssDNA outputs the fluorescent signal after cleavage [22]. This *trans*-cleavage activity endows CRISPR-Cas platforms with unexceptionable signal amplification ability Moreover, CRISPR-Cas system has combined with other amplification modes including rolling circle transcription, hybridization chain reaction, strand displacement amplification, and catalytic hairpin assembly [23–26]. In this work, CRISPR-Cas system is firstly coupled with DNAzyme walking nanomachine to output and amplify the signal.

Lipopolysaccharide (LPS) exists in the outer membrane of Gram-negative bacteria and mainly be made up of three regions including core polysaccharide, O-specific antigen and lipid A [27,28]. It is an extremely toxic inflammatory stimulator which is responsible for diarrhea, fever, septic shock, and even death [29,30]. Currently, limulus amebocyte lysate had been approved by international pharmacopoeias as the standard method to analyze LPS [31]. Whereas, it is highly sensitive to changes in pH values and temperature as well as other interfering factors [32]. Immunoassay has also been used for analysis of LPS, whereas it requires cumbersome preparation and detection procedure [33]. Furthermore, by using LPS-binding peptide or LPS aptamer [34,35], optical and electrochemical sensors have also been developed [29,32,36]. Among them, the simplest detection method is based on the characteristic of graphene oxide (GO) quenching the fluorescence [21]. LPS can result in the release of fluorophore labeled aptamer from the surface of GO and the following fluorescence recovery [36]. Meanwhile, LPS can induce the release of reported strand from the hybrid dual-strand formed by the aptamer and the signal probe, and the released signal probe can start the exonuclease III assisted terminal deoxynucleotidyl transferase amplification reaction [37]. Additionally, gold nanoparticle and copolythiophene-based LPS sensors have also been established [36,38,39]. Even so, it is still urgent to explore the robust and sensitive method for the analysis of LPS.

Herein, we present a hydrazone ligation assisted DNAzyme walking nanomachine coupled with CRISPR-Cas12a cascade amplification for LPS analysis. In our strategy, the full-length walking strand (AS) consists of two split segments, i. e. ASI and ASII, which are separately labeled by hydrazine group and aldehyde group, and the ASII is a DNAzyme strand locked by LPS aptamer. Competitive binding of LPS and its aptamer will lead to the release of ASII so as to trigger DNAzyme walking nanomachine. The product from DNAzyme walking nanomachine can activate collateral activity of Cas12a and trigger the further signal amplification. By combining of hydrazone ligation assisted DNAzyme walking nanomachine and CRISPR-Cas12a, the strategy can significantly improve the analytical sensitivity. The strategy could be considered as a general amplification platform for sensitive analysis of not only LPS but also other different biomolecules.

2. Materials and methods

2.1. Materials

1-(3-Dimethylaminopropyl)-3-ethylcarbodiimide hydrochloride (EDC) and *N*-hydroxysuccinimide (NHS) used to activate carboxyl group were from Sinopharm Chemical Reagent Beijing Co., Ltd (Beijing, China) and Shanghai Sangon Biotechnology Co., Ltd. (Shanghai, China), respectively. The reagents used in the specificity and anti-interference experiments were as follows: chitosan (CTS) were bought from Shanghai Sangon Biotechnology Co., Ltd., bovine serum albumin (BSA) were purchased from Sinopharm Chemical Reagent Beijing Co., Ltd., glucose (Glu), lactose (Lac), ovalbumin (Ova) were provided by Sigma-Aldrich (Shanghai, China). 4-Aminobenzoic hydrazide and LPS from *Escherichia coli* O55:B5 were also provided by Sigma-Aldrich. The EnGenLba Cas12a and RNase inhibitor used in CRISPR-Cas system and all the soft drinks needed in the real sample detection are from the same source as our previous published articles [40]. In this experiment, we used orange juice instead of grapefruit juice. Commercial ELISA kit was obtained from Shanghai Zhen Ke Biological Technology Co., Ltd. (Shanghai, China). Streptavidin coated magnetic beads (100 nm diameter) was bought from BioMag Biotechnology Co., Ltd (Wuxi, China). All the DNAs (see Table S1) were synthesized by Shanghai Sangon Biotechnology Co. Ltd.

2.2. Cascade signal amplification through hydrazone ligation assisted DNAzyme walking nanomachine coupled CRISPR-Cas12a

Firstly, EDC and NHS were dissolved in a ratio of 5:1.10 μL mixture and 20 μL carboxyl modified strand (0.12 μM) were reacted at room temperature for 15 min to activate the carboxyl group. Then, 20 μL 4-aminobenzoic hydrazide (6 μM) was further added and reacted at 37 °C for 3 h, followed by purification through GE filtration column (illustra™ MicroSpin™ G-25 Columns), to give the hydrazine modified ASI. Subsequently, ASI (0.12 μM) and SS (2.4 μM) were added to the magnetic bead and reacted at room temperature for 1 h to form the MB@SS/ASI. Then ASII (0.3 μM) was added to the system and reacted at 37 °C for 1.5 h. After washing, Mg^{2+} (20 mM) was added and reacted at 37 °C for 2 h. After washing, the supernatant was mixed with 10 × buffer, RNase inhibitor (80 U), Cas12a (30 nM), CrRNA (30 nM), and SS' (200 nM) for 35 min at 37 °C, and the Cas12a was inactivated at 65 °C for 10 min. The fluorescence analysis was carried out according to our previous report [7].

2.3. Characterization of analytical system

The formed hydrazone bonds were characterized by Fourier Transform Infrared Spectroscopy (FT-IR) according to our previous report [41]. In this experiment, ASI (0.12 μM) and ASII (0.3 μM) were reacted to give ASI-ASII in PBS buffer (pH 7.4). The whole experimental process was characterized through non-denaturing polyacrylamide gel electrophoresis (PAGE) [42]. In this experiment, the concentration of polyacrylamide used was 15% and the electrophoresis time was 1 h.

2.4. LPS analysis through cascade signal amplification

LPSA (5 μM) and ASII (5 μM) were mixed and heated to 95 °C for 5 min and gradually cooled to room temperature to form LPSA/ASII hybrid duplex. Subsequently, 10 μL LPSA/ASII was added into 10 μL LPS at different concentrations for 1.5 h at 37 °C, and the above 20 μL solution was added to the MB@SS/ASI at 37 °C for 1.5 h. After washing, Mg^{2+} (20 mM) was added into the system and reacted at 37 °C for 2 h. Finally, 10 × Buffer, RNase inhibitor (80 U), Cas12a (30 nM), CrRNA (30 nM) and SS' (200 nM) were added into the supernatant after separation for 35 min at 37 °C, and the Cas12a was inactivated at 65 °C for 10 min. The fluorescence of the obtained mixture was analyzed as above.

2.5. Analytical performance of the established method

Glu, Lac, Chi, BSA and Ova (5 mg/mL) were used instead of LPS (0.1 mg/mL) for specificity analysis. Then these samples (5 mg/mL) were mixed with LPS (0.1 mg/mL) respectively to evaluate the anti-interference ability of our method. In addition, different concentrations of LPS (100,000 ng/mL, 100 ng/mL and 1 ng/mL) were added into soft drinks to obtain spiked samples, which were analyzed by the established method.

3. Results and discussions

3.1. Hydrazone ligation assisted DNAzyme walking nanomachine coupled with CRISPR-Cas12a

The principle of hydrazone ligation assisted DNAzyme walking nanomachine coupled with CRISPR-Cas12a is depicted in Fig. 1A. AS strand is divided into ASI modified by hydrazine group and ASII modified by aldehyde group. The ASI and substrate strand (SS) containing a ribonucleobase (rA) cleavage site are conjugated onto the streptavidin coated magnetic beads (MBs) to form MB@SS/ASI. The further addition of ASII, which is a modified 8−17 DNAzyme, can cause the formation of the whole walking strand through hydrazone ligation. As shown in Fig. 1B, the new absorption peak at 1412 cm^{-1} is the characteristic peak of C═N, which indicates that ASI and ASII are successfully connected by hydrazone reaction. Meanwhile, a new band in lane 4 (top) also confirms the formation of the whole walking strand (Fig. 1C). The formed whole walking strand can form a partial duplex with the SS by complementary base pairing. Subsequently, DNAzyme-catalyzed cleavage of SS liberates the walking strand in the presence of Mg^{2+}, so that it can bind with another SS on the beads. As given in Figs. S1A and a new band appears after adding ASII, proving that the activation effect on DNAzyme and the resulting cleavage of SS. The cleavage of DNAzyme is the driving force for the walking strand to move autonomously along the track of MBs. The continuous cleavage of SS will lead to appearance of numerous product strand (PS) in the solution after magnetic separation. These PS can activate the *trans*-cleavage activity of Cas12a, causing the indiscriminate cleavage of the dual-labeled ssDNA fluorescence reporter (SS′) and the corresponding increase of the fluorescence intensity. We use SS'' that longer than SS′ to replace SS′ to verify the *trans*-cleavage activity. As shown in Fig. S1B, SS'' can be digested into random fragments in the presence of PS. Meanwhile, the fluorescence intensity increased after the addition of PS (Fig. S1C). Therefore, the fluorescence intensity is directly related with the concentration of the ASII.

As exhibited in Fig. 1C and 1D, the random fragments appear (lane 7) and high fluorescence intensity can be found (red curve) with ASII, respectively. It well confirms that high efficiency of hydrazone reaction initiates DNAzyme walking nanomachine and the following CRISPR-Cas12a *trans*-cleavage. In contrast, low fluorescence intensity can be observed (black curve) and there is no cleavage of SS'' in absence of ASII (lane 6). It can be explained for no occurrence of DNAzyme walking nanomachine and inactivation of Cas12a, because of no cleavage of SS by DNAzyme. These results well confirm that hydrazone ligation assisted DNAzyme walking nanomachine can couple with CRISPR-Cas12a to cause cascade signal amplification.

3.2. Mechanism investigation for LPS analysis through hydrazone ligation assisted DNAzyme walking nanomachine coupled with CRISPR-Cas12a

Hydrazone ligation assisted DNAzyme walking nanomachine coupled with CRISPR-Cas12a can be developed into a biosensor for the analysis of various targets. We have investigated it for the analysis of LPS. Fig. 2A illustrates the mechanism of LPS analysis through cascade signal amplification. LPS aptamer (LPSA) can firstly hybrid with ASII to form LPSA/ASII. As exhibited in Fig. 2B, the top band in lane 3 represents the LPSA/ASII duplex. Subsequently, the competitive combination of LPS and LPSA results in the release of ASII. As shown in Fig. 2B, the top band of LPSA/ASII in lane 4 is weaker than that in lane 3. After that, the released ASII can react with ASI immobilized on the modified MBs to give MB@SS/ASI/ASII. Then DNAzyme walking nanomachine happens to progressively cleave the SS strand and the produced PS can further activate *trans*-cleavage activity of Cas12a. Therefore, LPS can directly lead to the occurrence of high fluorescence.

As shown in Fig. 2B and 2C, the random fragment (Lane 7) and high fluorescence intensity (red curve) appears after the addition of LPS respectively, which indicates cascade signal amplification process initiated by LPS. On the contrary, there is no cleavage of SS'' (Lane 6). The corresponding fluorescence value is very low (black curve). This may be explained for the reason that LPSA/ASII has the ability to inhibit hydrazone reaction and prevent the cleavage of DNAzyme. These results well demonstrate the feasibility of LPS analysis.

3.3. Analysis of LPS through hydrazone ligation assisted DNAzyme walking nanomachine coupled with CRISPR-Cas12a

We have further utilized the developed method to quantitatively detect LPS content under the optimized conditions including binding time of LPS and LPSA/ASII, hydrazone reaction time, concentration ratio of ASI and SS on the surface of MBs (Figs. S2 and S3). As shown in Fig. 3A, fluorescence intensities gradually rise upon the addition of LPS at increasing concentrations. It can be explained for gradual release of ASII from hybridized LPSA/ASII induced by LPS binding. The released ASII can react with ASI on modified MBs surface through hydrazone bond to form MB@SS/ASI/ASII, followed by the production of PS to initiate CRISPR-Cas12a *trans*-cleavage on SS' and fluorescence recovery. As shown in Fig. 3B, the linear range of the fitting equation is 0.05 ng/mL to 10^6 ng/mL that is wider than previous reports [29,43]. Meanwhile, the detection limit is 7.31 fg/mL, lower than the previous report [31, 32, 44−46]. In addition, by using a FAM-labeled SS strand instead of SS strand, only DNAzyme walking nanomachine has been constructed to quantify LPS through directly detecting the fluorescence intensity of the supernatant after magnetic separation (Fig. S4). The calculated detection limit (34.10 fg/mL) was higher than that (7.31 fg/mL) of the constructed method. This indicates the high sensitivity of LPS analysis through hydrazone ligation assisted DNAzyme walking nanomachine coupled with CRISPR-Cas12a. In addition, the mean relative standard deviation (*RSD*) of the three experiments was 3.3%, which indicates that our method owns good reproducibility.

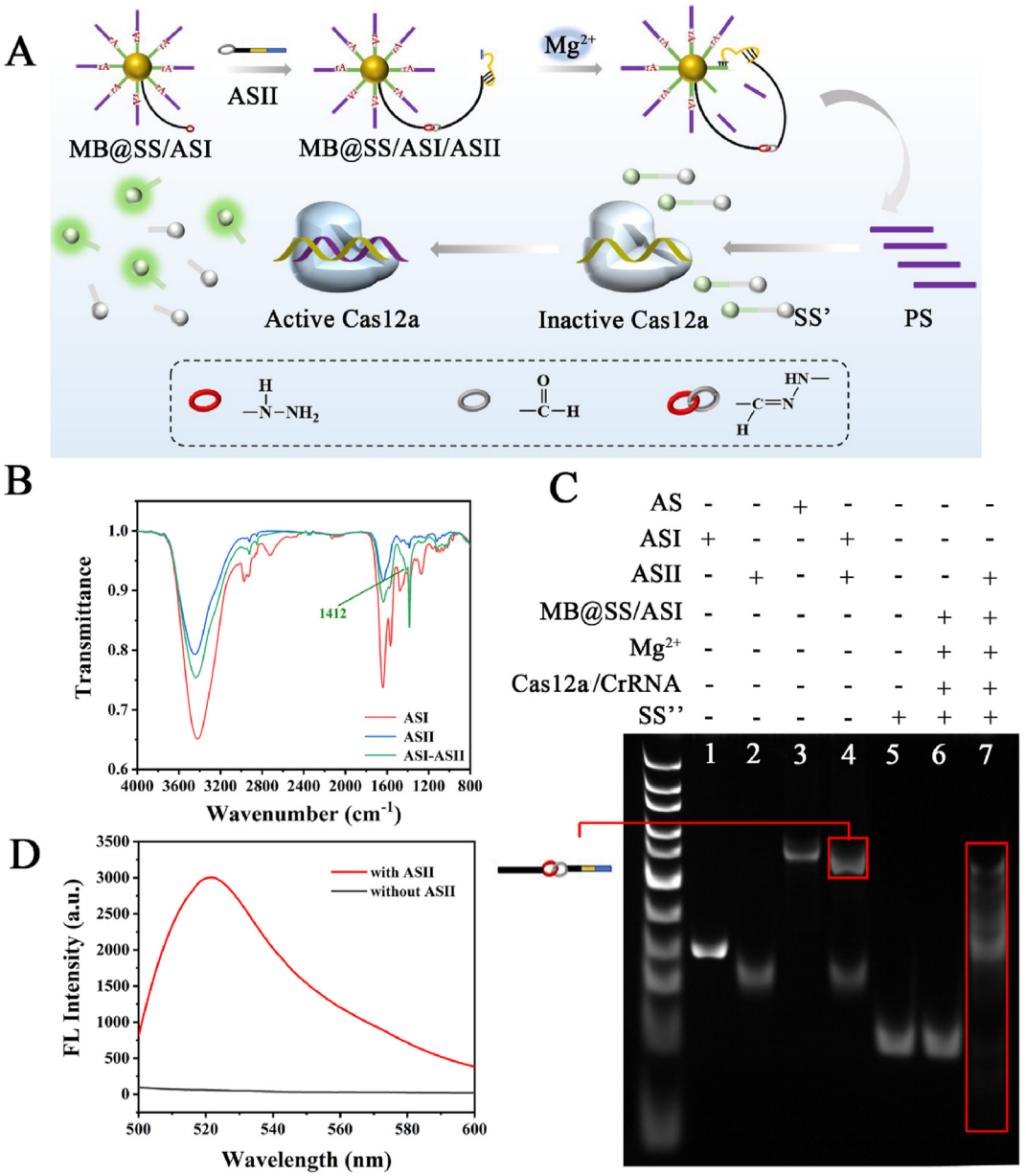


Fig. 1. (A) Schematic illustration for cascade signal amplification through hydrazone ligation assisted DNAzyme walking nanomachine coupled with CRISPR-Cas12a. (B) Fourier transform infrared spectra of ASI, ASII, and ASI-ASII. (C) Electropherogram for PAGE. (D) Fluorescence spectra of supernatant obtained with (red) and without (black) the addition of ASII. (For interpretation of the references to colour in this figure legend, the reader is referred to the Web version of this article.)

3.4. Analytical performance of the established method

To evaluate the specificity of the proposed method, LPS has been substituted with monosaccharide (Glu), disaccharide (Lac), polysaccharide (CTS), protein (BSA) and glycoprotein (Ova), and the results are shown in Fig. 4A and Fig. S5. It can be seen that only when LPS is added, there will be high fluorescence value. This may be due to the fact that the addition of LPS induces the departure of ASII to trigger the cascade signal amplification successfully. On the contrary, the fluorescence value of other samples very low, which can be explained for nearly no release of ASII. The result suggests that the constructed method has the high specificity.

Then, the above non-specific samples were mixed with LPS respectively to evaluate the anti-interference ability of the proposed method. As exhibited in Fig. 4B and Fig. S6. Like that for LPS, almost unchangeable fluorescence can be obtained for its mixtures with Glu, Lac, CTS, BSA, and Ova, suggesting no influence of these interfering substances on the binding of LPS with LPSA. These results well verify the good anti-interference ability of our method. Furthermore, the practicability of the proposed method is also studied. Different concentrations of LPS have been added to soft drinks to obtain spiked samples. Then the LPS concentrations of these spiked samples were analyzed, and the results are shown in Fig. 4C, Table S2 and Fig. S7. The recovery ratio varies in the range from 90% to 110% with the *RSD* values lower than 10%. The content of LPS in the sample has also been analyzed through the commercial ELISA kit, and the obtained results are basically consistent with the detection results of the proposed method. These results confirm that the developed method has good anti-interference ability, and can be well used for the analysis of targets in real samples.

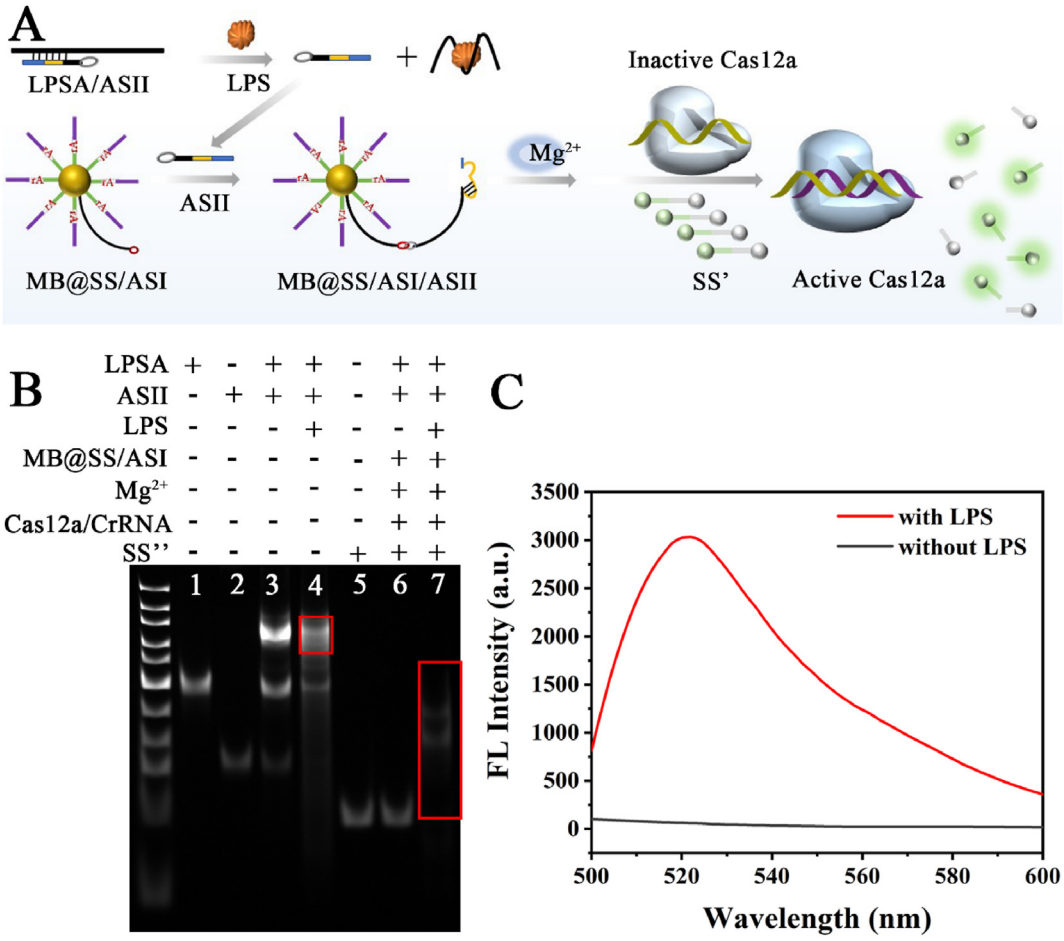


Fig. 2. (A) Schematic of the LPS analysis through cascade signal amplification. (B) Electropherogram for PAGE. (C) Fluorescence spectra with (red) and without (black) the addition of LPS. (For interpretation of the references to colour in this figure legend, the reader is referred to the Web version of this article.)

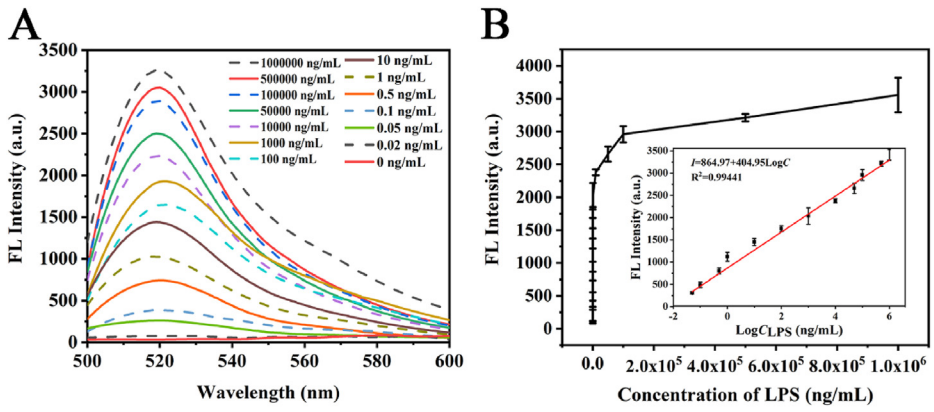


Fig. 3. (A) Fluorescence spectra in presence of different concentrations of LPS. (B) The changes of fluorescence intensities with different LPS concentrations. Inset displays the linear relationship of fluorescence variation against logarithmic values of LPS concentrations. Error bars show standard deviations of three independent measurements.

4. Conclusions

In conclusion, a novel signal output mode of hydrazone ligation assisted DNAzyme walking nanomachine is proposed. For the first time, hydrazone ligation assisted DNAzyme walking nanomachine is combined with CRISPR-Cas system for cascade signal amplification to quantitatively detect LPS. As one of the classical biorthogonal reactions, hydrazone ligation can assist the construction of DNAzyme walking nanomachine to couple with CRISPR-Cas12a. The sensitivity of the proposed method is greatly enhanced by dual signal amplification. Additionally, the established cascaded signal amplification platform broadens the application of CRISPR-Cas system in the field of bioanalysis.

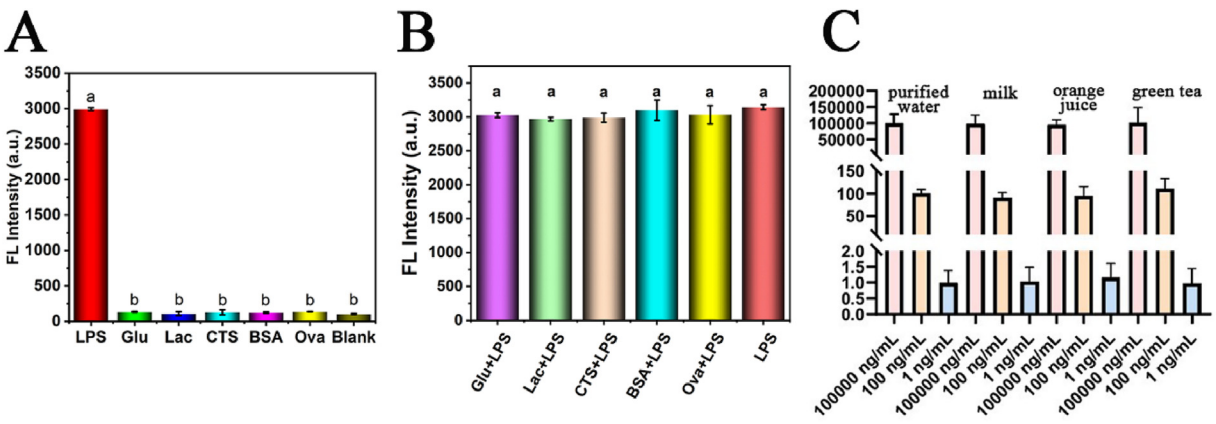


Fig. 4. (A) Specificity evaluation of the proposed method. The concentration of LPS is 100 μg/mL. The concentrations of other non-target samples were 5 mg/mL. (B) Anti-interference investigation of the proposed method. The concentration of LPS is 100 μg/mL. The concentrations of other non-target samples mixed with LPS were 5 mg/mL. (C) Real sample analysis for the proposed method. Error bars show standard deviations from three measurements.

CRediT authorship contribution statement

Pei Wang: Methodology, Conceptualization, Writing – original draft. **Yamei Liu:** Investigation, Resources. **Ying Yu:** Investigation, Visualization, Supervision. **Yuan Zhang:** Investigation, Data curation. **Jinhui Peng:** Investigation, Formal analysis. **Lili Niu:** Writing – review & editing. **Juan Zhang:** Funding acquisition, Writing – review & editing.

Declaration of competing interest

The authors declare that they have no known competing financial interests or personal relationships that could have appeared to influence the work reported in this paper.

Acknowledgements

This work is supported by the Science and Technology Commission of Shanghai Municipality (Grant Nos. 20392001800 and 20Y11912700), and National Natural Science Foundation of China (Grant No. 31671923).

Appendix A. Supplementary data

Supplementary data to this article can be found online at https://doi.org/10.1016/j.aca.2021.338747.

References

[1] K. Wang, M.Q. He, F.H. Zhai, J. Wang, R.H. He, Y.L. Yu, Autonomous DNA nanomachine based on cascade amplification of strand displacement and DNA walker for detection of multiple DNAs, Biosens. Bioelectron. 105 (2018) 159–165.
[2] C. Feng, Z. Wang, T. Chen, X. Chen, D. Mao, J. Zhao, G. Li, A dual-enzyme-assisted three-dimensional DNA walking machine using T4 polynucleotide kinase as activators and application in polynucleotide kinase assays, Anal. Chem. 90 (2018) 2810–2815.
[3] A.B. Chinen, C.M. Guan, J.R. Ferrer, S.N. Barnaby, T.J. Merkel, C.A. Mirkin, Nanoparticle probes for the detection of cancer biomarkers, cells, and tissues by fluorescence, Chem. Rev. 115 (2015) 10530–10574.
[4] C. Jung, P.B. Allen, A.D. Ellington, A simple, cleated DNA walker that hangs on to surfaces, ACS Nano 11 (2017) 8047–8054.
[5] M. Yang, X. Zhang, H. Liu, H. Kang, Z. Zhu, W. Yang, W. Tan, Stable DNA nanomachine based on duplex-triplex transition for ratiometric imaging instantaneous pH changes in living cells, Anal. Chem. 87 (2015) 5854–5859.
[6] P. Wang, T. Xue, A. Sheng, L. Cheng, J. Zhang, Application of chemoselective ligation in biosensing, Crit. Rev. Anal. Chem. (2020) 1–24.
[7] T. Xue, X. Yue, J. Wang, A. Sheng, P. Wang, J. Zhang, Self-assembly of DNA walker with biosensing application assisted by chemoselective ligation, Sens. Actuators, B 321 (2020) 128537.
[8] K. Yang, H. Wang, N. Ma, M. Zeng, H. Luo, D. He, Programmable target-initiated DNAzyme walker walking along a spatially isolated and highly hybridizable substrate track on a nanoparticle surface, ACS Appl. Mater. Interfaces 10 (2018) 44546–44553.
[9] X. Yang, Y. Tang, S.D. Mason, J. Chen, F. Li, Enzyme-powered three-dimensional DNA nanomachine for DNA walking, payload release, and biosensing, ACS Nano 10 (2016) 2324–2330.
[10] K. Wang, M.Q. He, F.H. Zhai, J. Wang, R.H. He, Y.L. Yu, Autonomous DNA nanomachine based on cascade amplification of strand displacement and DNA walker for detection of multiple DNAs, Biosens. Bioelectron. 105 (2018) 159–165.
[11] H.-B. Wang, L. Wang, K.-J. Huang, S.-P. Xu, H.-Q. Wang, L.-L. Wang, Y.-M. Liu, A highly sensitive and selective biosensing strategy for the detection of Pb^{2+} ions based on GR-5 DNAzyme functionalized AuNPs, New J. Chem. 37 (2013) 2557–2563.
[12] J.S. Chen, E. Ma, L.B. Harrington, M. Da Costa, X. Tian, J.M. Palefsky, J.A. Doudna, CRISPR-Cas12a target binding unleashes indiscriminate single-stranded DNase activity, Science 360 (2018) 436–439.
[13] E. Schunder, K. Rydzewski, R. Grunow, K. Heuner, First indication for a functional CRISPR/Cas system in francisella tularensis, Int. J. Med. Microbiol. 303 (2013) 51–60.
[14] J. Huang, Y. Wang, J. Zhao, CRISPR editing in biological and biomedical investigation, J. Cell. Physiol. 233 (2018) 3875–3891.
[15] H. Li, M. Li, Y. Yang, F. Wang, F. Wang, C. Li, Aptamer-linked CRISPR/Cas12a-Based immunoassay, Anal. Chem. 93 (2021) 3209–3216.
[16] M. Liang, Z. Li, W. Wang, J. Liu, L. Liu, G. Zhu, L. Karthik, M. Wang, K.-F. Wang, Z. Wang, J. Yu, Y. Shuai, J. Yu, L. Zhang, Z. Yang, C. Li, Q. Zhang, T. Shi, L. Zhou, F. Xie, H. Dai, X. Liu, J. Zhang, G. Liu, Y. Zhuo, B. Zhang, C. Liu, S. Li, X. Xia, Y. Tong, Y. Liu, G. Alterovitz, G.-Y. Tan, L.-X. Zhang, A CRISPR-cas12a derived biosensing platform for the highly sensitive detection of diverse small molecules, Nat. Commun. 10 (2019) 3672.
[17] Y. Li, H. Mansour, T. Wang, S. Poojari, F. Li, Naked-eye detection of grapevine red-blotch viral infection using a plasmonic CRISPR Cas12a assay, Anal. Chem. 91 (2019) 11510–11513.
[18] J. Li, S. Yang, C. Zuo, L. Dai, Y. Guo, G. Xie, Applying CRISPR-cas12a as a signal amplifier to construct biosensors for non-DNA targets in ultralow concentrations, ACS Sens. 5 (2020) 970–977.
[19] D. Zhang, Y. Yan, H. Que, T. Yang, X. Cheng, S. Ding, X. Zhang, W. Cheng, CRISPR/Cas12a-Mediated interfacial cleaving of hairpin DNA reporter for electrochemical nucleic acid sensing, ACS Sens. 5 (2020) 557–562.
[20] Y. Dai, R.A. Somoza, L. Wang, J.F. Welter, Y. Li, A.I. Caplan, C.C. Liu, Exploring the trans-cleavage activity of CRISPR-cas12a [cpf1] for the development of a universal electrochemical biosensor, Angew. Chem. Int. Ed. 58 (2019) 17399–17405.
[21] M. Xiao, W. Lai, T. Man, B. Chang, L. Li, A.R. Chandrasekaran, H. Pei, Rationally engineered nucleic acid architectures for biosensing applications, Chem. Rev. 119 (2019) 11631–11717.
[22] X. Yin, Z. Ding, H. Li, K. Zhao, Cooper, C. Liu, Dynamic aqueous multiphase reaction system for one-pot CRISPR-cas12a-based ultrasensitive and quantitative molecular diagnosis, Anal. Chem. 92 (2020) 8561–8568.
[23] G. Wang, W. Tian, X. Liu, W. Ren, C. Liu, New CRISPR-derived microRNA sensing mechanism based on Cas12a self-powered and rolling circle transcription-unleashed real-time crRNA recruiting, Anal. Chem. 92 (2020) 6702–6708.
[24] X. Hao, L. Zeng, Q. Mei, Y. Luo, Allosteric probe initiated wash-free method for sensitive extracellular vesicle detection through dual cycle-assisted CRISPR-cas12a, ACS Sens. 5 (2020) 2239–2246.

[25] S. Peng, Z. Tan, S. Chen, C. Lei, Z. Nie, Integrating CRISPR-cas12a with a DNA circuit as a generic sensing platform for amplified detection of MicroRNA, Chem. Sci. 11 (2020) 7362–7368.
[26] S. Yu, Y. Wang, L.P. Jiang, S. Bi, J.J. Zhu, Cascade amplification-mediated in situ hot-spot assembly for MicroRNA detection and molecular logic gate operations, Anal. Chem. 90 (2018) 4544–4551.
[27] B. Posha, H. Kuttoth, N. Sandhyarani, Layer-by-Layer assembly of polycations and polyanions for the sensitive detection of endotoxin, Langmuir 37 (2021) 257–265.
[28] L. Huang, H. Tao, S. Zhao, K. Yang, Q.Y. Cao, M. Lan, A tetraphenylethylene-based aggregation-induced emission probe for fluorescence turn-on detection of lipopolysaccharide in injectable water with sensitivity down to picomolar, Ind. Eng. Chem. Res. 59 (2020) 8252–8258.
[29] W.J. Shen, Y. Zhuo, Y.Q. Chai, R. Yuan, Cu-based metal-organic frameworks as a catalyst to construct a ratiometric electrochemical aptasensor for sensitive lipopolysaccharide detection, Anal. Chem. 87 (2015) 11345–11352.
[30] J. Niu, X. Hu, W. Ouyang, Y. Chen, S. Liu, J. Han, L. Liu, Femtomolar detection of lipopolysaccharide in injectables and serum samples using aptamer-coupled reduced graphene oxide in a continuous injection-electrostacking biochip, Anal. Chem. 91 (2019) 2360–2367.
[31] Z. Li, F. Luo, G. Dai, Y. Lu, S. Ai, P. He, Q. Wang, Microchip electrophoretic detection of bacterial lipopolysaccharide based on aptamer-modified magnetic beads and polymerase chain amplification, Microchem. J. 150 (2019) 104178.
[32] M. Pacheco, V.d. l. Asunción-Nadal, B. Jurado-Sánchez, A. Escarpa, Engineering janus micromotors with WS2 and affinity peptides for turn-on fluorescent sensing of bacterial lipopolysaccharides, Biosens. Bioelectron. 165 (2020) 112286.
[33] F.R. Lourenço, T.D.S. Botelho, T.D.J.A. Pinto, How pH, temperature, and time of incubation affect false-positive responses and uncertainty of the LAL gel-clot test, PDA J. Pharm. Sci. Technol. 66 (2012) 542–546.
[34] S.-E. Kim, W. Su, M. Cho, Y. Lee, W.-S. Choe, Harnessing aptamers for electrochemical detection of endotoxin, Anal. Chem. 424 (2012) 12–20.
[35] S. Voss, R. Fischer, G. Jung, K.-H. Wiesmüller, R. Brock, A fluorescence-based synthetic LPS sensor, J. Am. Chem. Soc. 129 (2007) 554–561.
[36] S.K. Lim, P. Chen, F.L. Lee, S. Moochhala, B. Liedberg, Peptide-assembled graphene oxide as a fluorescent turn-on sensor for lipopolysaccharide [endotoxin] detection, Anal. Chem. 87 (2015) 9408–9412.
[37] Y. Huang, L. Wang, L. Sha, Y. Wang, X. Duan, G. Li, Highly sensitive detection of lipopolysaccharide based on collaborative amplification of dual enzymes, Anal. Chim. Acta 1126 (2020) 31–37.
[38] P. Xie, L. Zhu, X. Shao, K. Huang, J. Tian, W. Xu, Highly sensitive detection of lipopolysaccharides using an aptasensor based on hybridization chain reaction, Sci. Rep. 6 (2016) 29524.
[39] J. Sun, J. Ge, W. Liu, X. Wang, Z. Fan, W. Zhao, H. Zhang, P. Wang, S.T. Lee, A facile assay for direct colorimetric visualization of lipopolysaccharides at low nanomolar level, Nano Res 5 (2012) 486–493.
[40] A. Sheng, P. Wang, J. Yang, L. Tang, F. Chen, J. Zhang, MXene coupled with CRISPR-cas12a for analysis of endotoxin and bacteria, Anal. Chem. 93 (2021) 4676–4681.
[41] T. Chen, A. Sheng, Y. Hu, D. Mao, L. Ning, J. Zhang, Modularization of three-dimensional gold nanoparticles/ferrocene/liposome cluster for electrochemical biosensor, Biosens. Bioelectron. 124–125 (2019) 115–121.
[42] A. Sheng, L. Su, J. Wang, T. Xue, P. Wang, J. Zhang, Hydrazone chemistry mediated toehold strand displacement cascade and its application for 5-hydroxymethylfurfural analysis, Anal. Chim. Acta 1104 (2020) 110–116.
[43] L. Kong, X. Zhou, G. Shi, Y. Yu, Molybdenum disulfide nanosheets-based fluorescent “off-to-on” probe for targeted monitoring and inhibition of β-amyloid oligomers, Analyst 145 (2020) 6369–6377.
[44] L.X. Wen, J.J. Lv, L. Chen, S.B. Li, X.J. Mou, Y. Xu, A fluorescent probe composed of quantum dot labeled aptamer and graphene oxide for the determination of the lipopolysaccharide endotoxin, Microchim. Acta 186 (2019) 122.
[45] Y. Tang, A. Kang, X. Yang, L. Hu, Y. Tang, S. Li, Y. Xie, Q. Miao, Y. Pan, D. Zhu, A robust OFF-ON fluorescent biosensor for detection and clearance of bacterial endotoxin by specific peptide based aggregation induced emission, Sens. Actuators, B 304 (2020) 127300.
[46] Z. Zhang, J. Yang, W. Pang, G. Yan, An aptamer-based fluorescence probe for facile detection of lipopolysaccharide in drinks, RSC Adv. 7 (2017) 54920–54926.